Superposition-state generation of nonorthogonal wavelike and particlelike states without ancillary qubits

Jian Li [1], Xiao-Xiao Chen [1], Zhe Meng [1], Jia-Zhi Yang [1], Qing-Yuan Wu [1], An-Ning Zhang [1,*] and Qing Zhao [1,2,†]

[1] *Center for Quantum Technology Research and Key Laboratory of Advanced Optoelectronic Quantum Architecture and Measurements (MOE), School of Physics, Beijing Institute of Technology, Haidian District, Beijing 100081, People's Republic of China*

[2] *Beijing Academy of Quantum Information Sciences, Beijing 100193, People's Republic of China*

(Received 8 November 2022; revised 28 December 2022; accepted 11 August 2023; published 28 August 2023)

The aim of this article is to generate the superposition state of nonorthogonal wavelike and particlelike states without ancillary qubits. Although it has been demonstrated that wavelike and particlelike states can be nonorthogonal, it remains unclear whether a superposition state of the two states can be achieved without the use of orthogonal ancillary qubits. To address this question, we employ a designed double-layer Mach-Zehnder interferometer that could continuously morph the single-photon state from particlelike to wavelike. Through both a theoretical analysis and experimental demonstration, we show that the nonorthogonality of wavelike and particlelike states can be maintained without ancillary qubits. The results showed that the two states are naturally nonorthogonal and can be directly utilized. As a variant of the delayed-choice experiment, our research will contribute to a deeper understanding of the nature of quantum objects, and also provide a different framework for discussions on wave-particle duality.

DOI: 10.1103/PhysRevA.108.022221

I. INTRODUCTION

Contrary to classical physics, quantum physics exhibits numerous peculiar phenomena. One characteristic that distinguishes it from classical physics is wave-particle duality. Bohr's complementarity principle suggests that a single quantum system can exhibit either wavelike or particlelike behavior, depending on the measurement apparatus [1]. This principle was subsequently demonstrated by Wheeler's delayed-choice gedanken experiment [2], which has been implemented in a variety of systems including photons, atoms, and superconducting circuits [3–10].

The superposition principle is another fascinating characteristic of quantum mechanics. By sending a quantum particle, such as a single photon, into a Mach-Zehnder interferometer (MZI) and controlling whether the interferometer is open or closed by ancillary qubits [11], some researchers have successfully prepared wave-particle superposition states [6,12–15].

Conversely, in linear algebra and quantum physics, states are often expanded in terms of an orthogonal set. The term "wave-particle duality" also implies that the wave state and the particle state are mutually exclusive. Research by Ionicioiu *et al.* [11] suggests that these two states can be nonorthogonal. However, Ionicioiu *et al.*'s theoretical framework [11] and subsequent series of experiments [5,6,12–15] still use orthogonal or nearly orthogonal ancillary qubits to generate wave-particle superposition states.

Is it possible to prepare nonorthogonal wavelike and particlelike states, as well as their superposition states, without using ancillary qubits? Research by Guo *et al.* proposed a theoretical scheme [16]. However, no experiments have been done to generate such wave-particle superposition states without the use of auxiliary qubits. By designing a double-layer Mach-Zehnder interferometer (DMZI), we proposed a theoretical scheme to achieve the generation of a wave-particle superposition state with adjustable expansion coefficients, and corresponding experiments have been conducted. Theoretical calculations and experimental results showed that nonorthogonal wavelike and particlelike states, as well as wave-particle superposition states, can be generated without using ancillary qubits. We also conducted a postselection experiment to demonstrate this. As a variant of the delayed-choice experiment, our scheme is compatible with the delayed choice experiment. By constructing a larger interferometer or using faster optical modulators, a complete delayed-choice experiment can be achieved.

II. DOUBLE-LAYER MACH-ZEHNDER INTERFEROMETER

Feynman said, "When alternatives cannot possibly be resolved by any experiment, they always interfere [17]," indicating that for a single-photon interferometer, a photon will interfere with itself when we cannot possibly tell which path the photon has chosen (wavelike behavior). However, when the path choice can be determined, the photon would no longer be able to interfere with itself (particlelike behavior).

In the aforementioned scenarios, the observer perceives two distinct states of the observed photons: wavelike and particlelike states. In the context of a Mach-Zehnder interferometer (MZI), the presence or absence of the second beam splitter impacts the wave-particle duality exhibited by photons. The crucial differentiating factor between the wavelike

[*] anningzhang@bit.edu.cn
[†] qzhaoyuping@bit.edu.cn

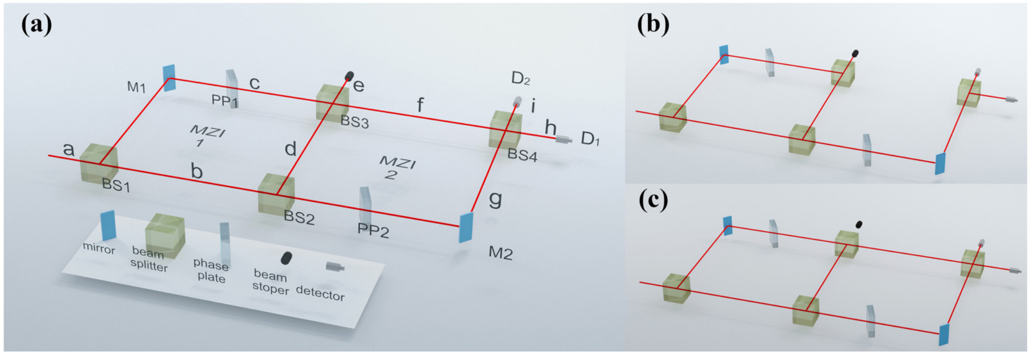

FIG. 1. Diagrams showing the DMZI under different conditions. (a) The path distribution of photons when a single-photon state is prepared into a wave-particle superposition state. (b) The path distribution of photons when a single-photon state is prepared into a particlelike state. Here, the MZI2 is incomplete because of the lack of the probability of photons passing along the path f. (c) The path distribution of photons when a single-photon state is prepared into a wavelike state. Conversely, the MZI2 is complete, with a phase shift introduced by the PP2 so that the single photon will be wavelike.

and particlelike states lies in whether the phase inside the interferometer affects the detection probability. In previous research [3,11], the wavelike state typically refers to the state described by $e^{i\frac{\varphi}{2}}(\cos\frac{\varphi}{2}|0\rangle - i\sin\frac{\varphi}{2}|1\rangle)$. In this state, the value of the phase φ has an impact on the detection probabilities of $|0\rangle$ and $|1\rangle$. On the other hand, the particlelike state refers to the state given by $\frac{1}{\sqrt{2}}(|0\rangle + e^{i\varphi}|1\rangle)$. In this state, the detection probabilities are not influenced by φ. In particular, when the second beam splitter is a quantum beam splitter and is in a superposition of being present and absent, the state of a single photon will also be in a superposition state of wavelike and particlelike states, known as a wave-particle superposition state [11].

We designed a type of interferometer (DMZI) to observe the wave-particle duality of a single photon, whose diagram is shown in Fig. 1. Notably, the DMZI is composed of two connected MZIs, from where by adjusting the phase shift between the two paths of MZI1, we could control whether the single photon in MZI2 will be distributed along one or both paths, thereby achieving a continuous morphing between them.

The path distribution of the particlelike state is illustrated in Fig. 1(b). By adjusting the phase shift φ_1 introduced by phase plate 1 (PP1), the photon was brought into a destructive interference condition along the path f after passing through MZI1. Consequently, every photon detected at detector 1 (D1) and D2 originates from the path g, thereby preventing interference. In this case the photon state in front of D1 and D2 corresponds to the particlelike state [6,11–14],

$$|\text{particle}\rangle = \tfrac{1}{2}ie^{-i\varphi_2}|h\rangle + \tfrac{1}{2}e^{-i\varphi_2}|i\rangle, \tag{1}$$

where $|h\rangle$ and $|i\rangle$ are the final paths h and i in Fig. 1(a). In previous research [6,11–14], the particlelike state exhibits a notable feature: The single-photon detection probability remains unaffected by the phase shift (denoted as φ_2 in our approach, introduced by the PP2). However, in our approach, there is a slight difference in which the detection probabilities of the particle state at detectors D1 and D2 are $\frac{1}{4}$ instead of the expected $\frac{1}{2}$.

On the other hand, the path distribution of the wavelike state is shown in Fig. 1(c). By adjusting φ_1, the photon was in the constructive interference condition along path f. However, for MZI2, paths f and g were recombined after beam splitter 4 (BS4), and the subsequent detection of the photon's which-path information at D1 and D2 remains unknown. Thus, similar to other research [6,11–14], the detection probability of D1 and D2 is dependent on φ_2. In this case, the photon state was the wavelike state:

$$|\text{wave}\rangle = \tfrac{1}{2}(ie^{-i\varphi_2} - 1)|h\rangle + \tfrac{1}{2}(e^{-i\varphi_2} - i)|i\rangle. \tag{2}$$

With intermediate cases after crossing the DMZI, the photon state was as shown below:

$$\Psi_{12} = \tfrac{1}{4}(ie^{-i\varphi_1} - 1 + 2ie^{-i\varphi_2})|h\rangle + \tfrac{1}{4}(2e^{-i\varphi_2} - e^{-i\varphi_1} - i)|i\rangle. \tag{3}$$

Notably, by expanding the photon state under the basis $\{|\text{particle}\rangle, |\text{wave}\rangle\}$, Eq. (3) becomes

$$\Psi_{12} = \frac{1 - ie^{-i\varphi_1}}{2}|\text{wave}\rangle + \frac{1 + ie^{-i\varphi_1}}{2}|\text{particle}\rangle, \tag{4}$$

where the terms $\frac{1-ie^{-\varphi_1}}{2}$ and $\frac{1+ie^{-\varphi_1}}{2}$ are the expansion coefficients. For more details, see the Supplemental Material [18] Sec. SI. From Eq. (4) while it was evident that the photon state was a wave-particle superposition state, by adjusting φ_1 from $-\frac{1}{2}\pi$ to $\frac{1}{2}\pi$, a continuous transition from the wavelike to the particlelike state was realized. The theoretical detection probabilities of D1 and D2 as a function of φ_1 and φ_2 are shown in Figs. 2(a) and 2(b). When $\varphi_1 = -\frac{1}{2}\pi$, the detection probability exhibits a sinusoidal oscillation with respect to φ_2, corresponding to the wavelike behavior. Conversely, when $\varphi_1 = \frac{1}{2}\pi$, the detection probability remains unaffected by changes in φ_2, which corresponds to the particlelike behavior. Therefore, our findings completed the generation of wavelike and particlelike states and superposition states, as in other research [6,12–14,19]. With DMZI, we achieved morphing between nonorthogonal wavelike and particlelike states without ancillary qubits. The nonorthogonality will be discussed in Sec. III. Furthermore, for different φ_1, the maximum and minimum detection probabilities of D1 and D2 occurred at different φ_2. For example, the solid red line and the solid blue line in Fig. 2(b) were respectively $\varphi_2 = \frac{1}{2}(\varphi_1 + 2.5\pi \pm \pi)$, which are the minimum and maximum theoretical detection

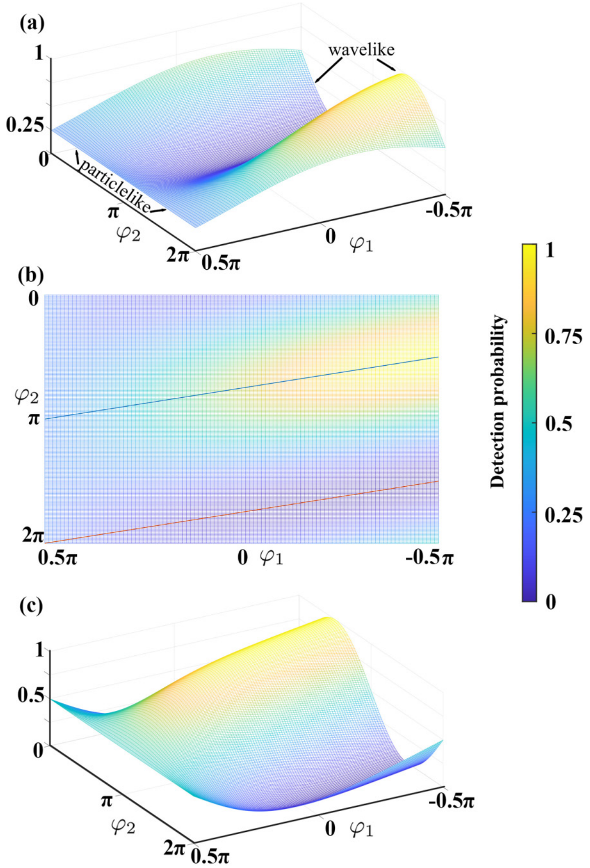

FIG. 2. Theoretical detection probability. (a) and (b) The theoretical detection probabilities of D1 and D2, equal to the square modulus of the coefficient of the $|h\rangle$ and the $|i\rangle$ basis in Eq. (3). As φ_1 changed from $-\frac{1}{2}\pi$ to $\frac{1}{2}\pi$, a wave-particle morphing could be observed at the two detectors. Except for the completely wavelike state, the sum of the two detection probabilities will be smaller than 1 due to the loss of the photon controlled by φ_1. (c) The theoretical detection probability of D2 renormalized to the sum of the two detection probabilities with the same φ_1 and φ_2. Especially, the peak or the dip will be at different φ_2 as the φ_1 changing.

probabilities of D2. In previous works [6,12–14,19], they appeared at a fixed φ_2.

Notably, this DMZI is a non-Hermitian system that allows for the introduction of phase-dependent losses. However, to get a Hermitian Hamiltonian, renormalizing the detection probabilities is needed [see Fig. 2(c)]. Nevertheless, our investigation confirms that utilizing the non-Hermitian Hamiltonian remains a viable approach for elucidating the nonorthogonality between the wavelike and particlelike states. It is important to highlight that the introduction of a non-Hermitian Hamiltonian breaks the symmetry between φ_1 and φ_2. In our proposed scheme, when φ_1 is equal to $\frac{1}{2}\pi$ or $-\frac{1}{2}\pi$, the single-photon state can be seen as a particlelike state or wavelike state dependent on φ_2. However, it is not possible to find a fixed φ_2 that would make the single-photon state a particlelike state or wavelike state dependent on φ_1. In previous research, both wavelike and particlelike behaviors could be observed along two distinct variables. However, in our proposed scheme with a non-Hermitian Hamiltonian, the relationship between the variables φ_1 and φ_2 is not symmetric, leading to a different behavior compared to previous schemes. For more details about the non-Hermitian Hamiltonian and the asymmetry, see the Supplemental Material [18] Sec. SII. Furthermore, we believe that the revelation of the nonorthogonality of wave-particle duality can have an impact on the discussion of non-Hermitian systems, as nonorthogonal eigenstates are widely used in such discussions [20,21].

III. NONORTHOGONALITY BETWEEN WAVELIKE AND PARTICLELIKE STATES

The generation of wave-particle superposition using DMZI has a property: The phase rather than the polarization controls the expansion coefficients of $|\text{particle}\rangle$ and $|\text{wave}\rangle$. Most previous research has been performed with the introduction of orthogonal ancillary states (e.g., orthogonal polarization) [6,9,12–15,22,23] that correspond to the wavelike and particlelike states. However, the DMZI controlled the interferometer by adjusting φ_1, without introducing the orthogonal ancillary states, indicating that when the wavelike and particlelike states do not need to be encoded on orthogonal polarizations, the nonorthogonality of the two states could be revealed.

We obtained the scalar product of $|\text{particle}\rangle$ and $|\text{wave}\rangle$ from Eqs. (1) and (2):

$$\langle \text{particle}|\text{wave}\rangle = \tfrac{1}{2} \neq 0. \tag{5}$$

This situation is different from other research [6,12–14,19]. In previous research, these two states were encoded on two orthogonal states of ancillary qubits. When wavelike behavior dominates, the ancillary qubit is in a specific state (e.g., vertical polarization), and the other orthogonal state (e.g., horizontal polarization) correlated with the particlelike state disappears, and vice versa. However, our theory and the following experiments show that when the quantum particle is in a wavelike state, it could be decomposed into a superposition of particlelike states and vice versa. In other words, they are naturally not orthogonal.

Based on the above findings, this article subsequently demonstrates this nonorthogonality using a postselection operation (see the Supplemental Material [18] Sec. SIII). The $|\Psi_{\text{post}}\rangle$ here is $|\text{particle}\rangle$, and we choose the $|\text{wave}\rangle$ to be the $|\Psi_{\text{pre}}\rangle$. Then the detection probability p_{post} was calculated using the expression below:

$$p_{\text{post}} = |\langle \Psi_{\text{post}}|\Psi_{\text{pre}}\rangle|^2 = |\langle \text{particle}|\text{wave}\rangle|^2. \tag{6}$$

If p_{post} is not equal to zero, it proves that the $|\text{wave}\rangle$ and $|\text{particle}\rangle$ are not orthogonal.

After parametrizing φ_2, our investigations revealed that the particlelike and wavelike states were linearly dependent, as proved in Supplemental Material [18] Sec. SIV.

IV. EXPERIMENT DEMONSTRATION

The experimental setup was divided into three parts: First, a heralded single-photon source (HSPS) was used to generate single photons [shown in Fig. 3(a)], where a 405-nm continuous-wave laser was made to go through a periodically poled potassium titanyl phosphate crystal (PPKTP) to

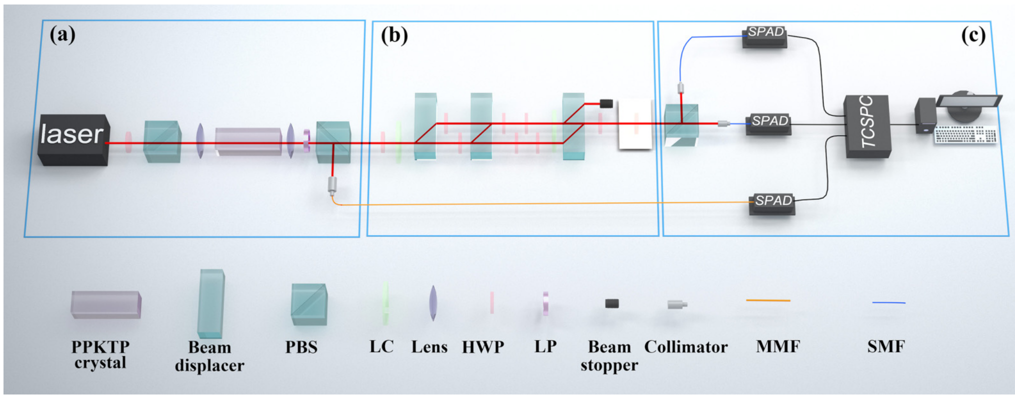

FIG. 3. The experimental setup. (a) The HSPS. (b) The experimental setup for the single-photon DMZI and the unitary transformation of the postselection operation. (c) The detection part. PBS: polarization beam splitter; LC: liquid-crystal device; HWP: half-wave plate; LP: long-pass filter; MMF: multimode fiber; SMF: single-mode fiber.

generate a pair of entangled photons via the type-II spontaneous parametric down-conversion (SPDC) process. Subsequently, one of the photons was transmitted at the polarization beam splitter (PBS), acting as a signal photon, and the other photon was reflected, acting as a trigger photon.

Second, the experimental DMZI and the unitary transformation of the postselection operation, realizing the proposed scheme of Fig. 1 and Sec. III, is displayed in Fig. 3(b). Notably, the signal photon was incident from the upper left. Then, beam displacers (BDs) were used to build the DMZI, after which two liquid-crystal devices (LCs) were used to adjust the phase shift. While the angle of the half-wave plates (HWPs) before the first BD was 30°, from left to right, the angles of the three HWPs in the upper path, located between the first and the final BDs in Fig. 3(b), were (45°, 22.5°, and 45°), the angles of the three HWPs in the lower path were (72.4°, 45°, and 0°), and the angle of the HWP after the final BD was 22.5°. Then, unitary transformations of the postselection operation were done using an extra HWP at 22.5° [the ivory part in Fig. 3(b)], which was put only when a postselection was performed, indicating that this HWP could map $|\text{particle}'\rangle$ to $\frac{1}{\sqrt{2}}|H\rangle$ (the prime $'$ indicates the experimental setup).

Finally, Fig. 3(c) shows the detection part of the experiment. Three single-photon avalanche diodes (SPADs) were used to receive the photons: The SPAD at the bottom of the three was used to receive the trigger photons, the middle SPAD corresponded to detector D_1', and the top one corresponded to D_2'. For more details, see the Supplemental Material [18] Secs. SV–SVIII.

As a result, the scalar product of $|\text{particle}'\rangle$ and $|\text{wave}'\rangle$ was obtained, as shown below:

$$\langle \text{particle}'|\text{wave}'\rangle = \tfrac{1}{2}. \tag{7}$$

Evidently, the experimental setup faithfully implemented the scheme in the theory part.

V. RESULTS

Experiments were performed on each of the two detectors (D1 and D2) after BS4 with 20 equally spaced φ_1' in $[0, \pi]$ and 40 equally spaced φ_2' in $[0, 2\pi]$ to prove the existence of the wave-particle superposition state. Thus 1600 results were obtained with an average photon number about 46 000. Furthermore, each MZI comprised two BDs carefully tuned so that no additional phase is generated between the two paths of the interferometer. As a result, we discovered the visibility of the DMZI to be 99.3% at maximum.

In Figs. 4(a) and 4(b), experimental data points were represented as dots while we plotted the ideal conditional detection probability as a function of φ_1 and φ_2 in the form of a color mesh. Figure 4 shows that the photon state at D1 and D2 could simultaneously morph from a wavelike to a particlelike behavior.

Next, we used one more parameter to demonstrate this morphing. Since the visibility (Vis) and the path distinguishability (Dis) are often discussed in the study of the wave-particle superposition state, and Bohr's complementarity

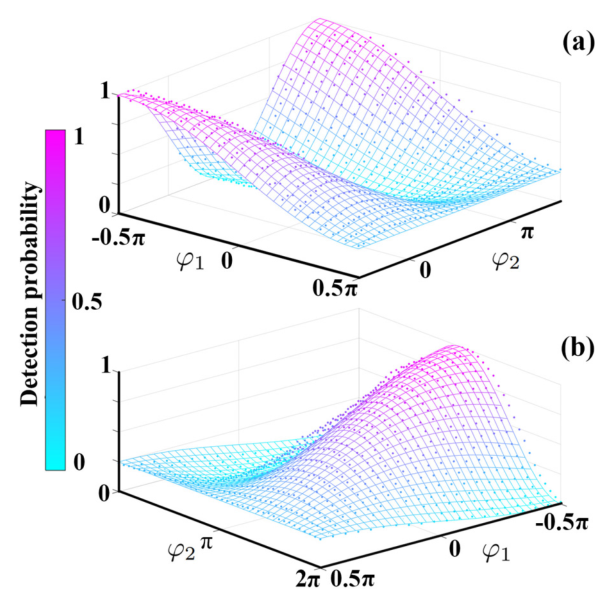

FIG. 4. Experimental results of the detection probability at (a) D_1' and (b) D_2'. While the color mesh shows the theoretical results, the points are the experimental results. For clarity, the horizontal and vertical coordinates were denoted φ_1 and φ_2, where the correspondence between φ_1' φ_2' and φ_1 φ_2 could be seen in the Supplemental Material [18] Sec. SVII.

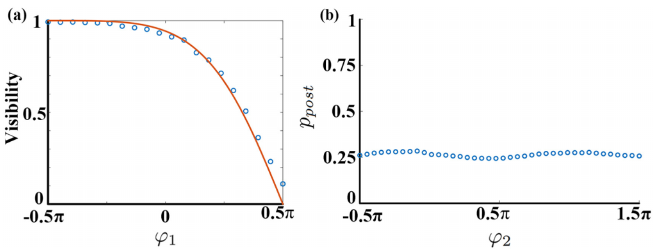

FIG. 5. (a) The relationship between visibility and φ_1. The orange line shows the theoretical curve, and the blue circles denote the result of the experiments. (b) p_{post} obtained from the experiment results with different φ_2. According to Eq. (6), the theoretical p_{post} was always equal to $\frac{1}{4}$ for the $|\text{wave}\rangle$ with a different φ_2, where, for clarity, the horizontal and vertical coordinates were denoted φ_1 and φ_2.

principle gives an inequality relation satisfied between the Vis and the Dis [24,25], the inequality relation has been further investigated in many studies [23,26–29]. Hence, we choose Vis from our findings to indicate how wavelike is a photon state. As shown in Fig. 5(a), by varying φ_1, Vis changed from 1 to 0, showing the photon's wave-to-particle transition, indicating that wavelike behavior was fading as the φ_1 changed from $-\frac{1}{2}\pi$ to $\frac{1}{2}\pi$.

The detection probability after postselection is shown in Fig. 5(b). Investigations revealed that p_{post} was significantly not equal to 0, indicating that our experimental device encoded the states of wavelike and particlelike behavior states into nonorthogonal states without ancillary states, and the orthogonal coding of wavelike and particlelike behavior states was unnecessary.

VI. DISCUSSION

The wave-particle duality has sparked widespread discussion [14,19,30–33]. The theoretical scheme for generating wave-particle superposition states using an MZI and ancillary qubit has been proposed [11]. Several experiments have been conducted based on this scheme [5,6,12–15]. In addition, theories based on wave-particle superposition states have been widely discussed, including the relationship between wave-particle duality and hidden variable theory, the retrocausality, and the entanglement [23,29]. In particular, by introducing the prepare-and-measure scenario, a modified Wheeler experiment can rule out the classical two-dimensional hidden variable theory in a device-independent way [34], and experiments based on this theory have been done [35,36]. Overall, the generation of wave-particle superposition states provides a means to investigate the fundamental quantum mechanical problem of wave-particle duality.

We present a method for generating wave-particle superposition states, without the use of ancillary qubits, and experimentally implement it. In addition, we demonstrate the nonorthogonality of the generated wavelike and particlelike states through a postselection experiment. Our approach offers a more comprehensive manifestation of the nonorthogonality between wavelike and particlelike states by eliminating the need for orthogonal auxiliary qubits. This absence of orthogonal auxiliary qubits enables a more direct and focused exploration of the relationship between the two states. We believe that our method can be combined with the prepare-and-measure scenario to obtain a modified DMZI that can enrich the discussion on wave-particle duality and hidden variable theory. Notably, our approach, which incorporates DMZI, produces differences in the properties of wave-particle superposition states that contrast with previous theoretical results [11], including a distinct relationship between the maximum detection probability and phase. In the context of wave-particle duality, it is essential to exercise caution due to the presence of nonorthogonality, since, depending on the measurement apparatus, one of the wavelike or the particlelike nature will dominate. Still, this event does not mean that the other one disappears. Hence, the wavelike and the particlelike natures as intrinsic properties of quantum particles are consistent with the existence of quantum particles.

It is worth noting that our DMZI is a non-Hermitian system. Unlike other research, the symmetry of the two parameters that enable the continuous morphing between wavelike and particlelike states is broken. Given the widespread use of nonorthogonal eigenstates in non-Hermitian systems, we are curious as to whether wave-particle duality can be proven to be a fundamental characteristic in non-Hermitian systems. As the MZI has already been widely applied in different systems [37–41], we hope that our approach can serve as a basis for future research on wave-particle duality and non-Hermitian physics in various systems.

ACKNOWLEDGMENTS

We are grateful to Prof. O. C. Hiap and Prof. S.-W. Li for their useful discussions. This work is supported by the National Natural Science Foundation of China (Grant No. 92365115).

[1] *Quantum Theory and Measurement*, edited by J. A. Wheeler and W. H. Zurek (Princeton University Press, Princeton, NJ, 2014).

[2] J. A. Wheeler, The "past" and the "delayed-choice" double-slit experiment, in *Mathematical Foundations of Quantum Theory*, edited by A. Marlow (Academic Press, New York, 1978), pp. 9–48.

[3] A. Peruzzo, P. Shadbolt, N. Brunner, S. Popescu, and J. L. O'Brien, A quantum delayed-choice experiment, Science **338**, 634 (2012).

[4] A. G. Manning, R. I. Khakimov, R. G. Dall, and A. G. Truscott, Wheeler's delayed-choice gedanken experiment with a single atom, Nat. Phys. **11**, 539 (2015).

[5] K. Liu, Y. Xu, W. T. Wang, S. B. Zheng, T. Roy, S. Kundu, M. Chand, A. Ranadive, R. Vijay, Y. Song, L. Duan, and L. Sun, A twofold quantum delayed-choice experiment in a superconducting circuit, Sci. Adv. **3**, e1603159 (2017).

[6] J. S. Tang, Y. L. Li, X. Y. Xu, G. Y. Xiang, C. F. Li, and G. C. Guo, Realization of quantum Wheeler's delayed-choice experiment, Nat. Photonics **6**, 600 (2012).

[7] M. X. Dong, D. S. Ding, Y. C. Yu, Y. H. Ye, W. H. Zhang, E. Z. Li, L. Zeng, K. Zhang, D. C. Li, G. C. Guo, and B. S. Shi, Temporal Wheeler's delayed-choice experiment based on cold atomic quantum memory, npj Quantum Inf. **6**, 72 (2020).

[8] X. S. Ma, J. Kofler, and A. Zeilinger, Delayed-choice gedanken experiments and their realizations, Rev. Mod. Phys. **88**, 015005 (2016).

[9] V. Jacques, E. Wu, F. Grosshans, F. Treussart, P. Grangier, A. Aspect, and J. F. Roch, Experimental realization of Wheeler's delayed-choice gedanken experiment, Science **315**, 966 (2007).

[10] T. Hellmuth, H. Walther, A. Zajonc, and W. Schleich, Delayed-choice experiments in quantum interference, Phys. Rev. A **35**, 2532 (1987).

[11] R. Ionicioiu and D. R. Terno, Proposal for a Quantum Delayed-Choice Experiment, Phys. Rev. Lett. **107**, 230406 (2011).

[12] F. Kaiser, T. Coudreau, P. Milman, D. B. Ostrowsky, and S. Tanzilli, Entanglement-enabled delayed-choice experiment, Science **338**, 637 (2012).

[13] K. Wang, Q. Xu, S. Zhu, and X. S. Ma, Quantum wave–particle superposition in a delayed-choice experiment, Nat. Photonics **13**, 872 (2019).

[14] A. S. Rab, E. Polino, Z. X. Man, N. Ba An, Y. J. Xia, N. Spagnolo, R. Lo Franco, and F. Sciarrino, Entanglement of photons in their dual wave-particle nature, Nat. Commun. **8**, 915 (2017).

[15] W. Zhang, D. S. Ding, M. X. Dong, S. Shi, K. Wang, G. C. Guo, and B. S. Shi, Wave-particle superposition of distinct atomic spin excitations, Phys. Rev. A **98**, 063829 (2018).

[16] Q. Guo, W.-J. Zhang, G. Li, T. Zhang, H.-F. Wang, and S. Zhang, Modified quantum delayed-choice experiment without quantum control or entanglement assistance, Phys. Rev. A **104**, 022210 (2021).

[17] R. P. Feynman, A. R. Hibbs, and D. F. Styer, *Quantum Mechanics and Path Integrals* (Courier Corporation, North Chelmsford, NJ, 2010).

[18] See Supplemental Material at http://link.aps.org/supplemental/10.1103/PhysRevA.108.022221 for the theoretical derivation; non-Hermitian system with phase-dependent loss; the postselection operation in theory; state preparation, state evolution, and state measurement in experiment; the postselection operation in experiment; correspondence between theory and experiment; and the experimental equipment and experimental setup.

[19] B. Zhang, D. Ran, R. Ianconescu, A. Friedman, J. Scheuer, A. Yariv, and A. Gover, Quantum Wave-Particle Duality in Free-Electron–Bound-Electron Interaction, Phys. Rev. Lett. **126**, 244801 (2021).

[20] Y. Ashida, Z. Gong, and M. Ueda, Non-Hermitian physics, Adv. Phys. **69**, 249 (2020).

[21] M. Naghiloo, M. Abbasi, Y. N. Joglekar, and K. W. Murch, Quantum state tomography across the exceptional point in a single dissipative qubit, Nat. Phys. **15**, 1232 (2019).

[22] V. Jacques, E. Wu, F. Grosshans, F. Treussart, P. Grangier, A. Aspect, and J.-F. Roch, Delayed-Choice Test of Quantum Complementarity with Interfering Single Photons, Phys. Rev. Lett. **100**, 220402 (2008).

[23] R. Ionicioiu, R. B. Mann, and D. R. Terno, Determinism, Independence, and Objectivity are Incompatible, Phys. Rev. Lett. **114**, 060405 (2015).

[24] B. G. Englert, Fringe Visibility and Which-Way Information: An Inequality, Phys. Rev. Lett. **77**, 2154 (1996).

[25] G. Jaeger, A. Shimony, and L. Vaidman, Two interferometric complementarities, Phys. Rev. A **51**, 54 (1995).

[26] T. J. Herzog, P. G. Kwiat, H. Weinfurter, and A. Zeilinger, Complementarity and the Quantum Eraser, Phys. Rev. Lett. **75**, 3034 (1995).

[27] M. N. Bera, T. Qureshi, M. A. Siddiqui, and A. K. Pati, Duality of quantum coherence and path distinguishability, Phys. Rev. A **92**, 012118 (2015).

[28] B. Kanseri and Sethuraj K. R., Experimental observation of the polarization coherence theorem, Opt. Lett. **44**, 159 (2019).

[29] X. F. Qian, A. N. Vamivakas, and J. H. Eberly, Entanglement limits duality and vice versa, Optica **5**, 942 (2018).

[30] G. L. Long, W. Qin, Z. Yang, and J. L. Li, Realistic interpretation of quantum mechanics and encounter-delayed-choice experiment, Sci. China: Phys., Mech. Astron. **61**, 030311 (2018).

[31] S. Yu, Y. N. Sun, W. Liu, Z. D. Liu, Z. J. Ke, Y. T. Wang, J. S. Tang, C. F. Li, and G. C. Guo, Realization of a causal-modeled delayed-choice experiment using single photons, Phys. Rev. A **100**, 012115 (2019).

[32] R. Menzel, D. Puhlmann, A. Heuer, and W. P. Schleich, Wave-particle dualism and complementarity unraveled by a different mode, Proc. Natl. Acad. Sci. USA **109**, 9314 (2012).

[33] Y. Cao, Y. H. Li, Z. Cao, J. Yin, Y. A. Chen, H. L. Yin, T. Y. Chen, X. F. Ma, C. Z. Peng, and J. W. Pan, Direct counterfactual communication via quantum Zeno effect, Proc. Natl. Acad. Sci. USA **114**, 4920 (2017).

[34] R. Chaves, G. B. Lemos, and J. Pienaar, Causal Modeling the Delayed-Choice Experiment, Phys. Rev. Lett. **120**, 190401 (2018).

[35] H.-L. Huang, Y.-H. Luo, B. Bai, Y.-H. Deng, H. Wang, Q. Zhao, H.-S. Zhong, Y.-Q. Nie, W.-H. Jiang, X.-L. Wang, J. Zhang, L. Li, N.-L. Liu, T. Byrnes, J. P. Dowling, C.-Y. Lu, and J.-W. Pan, Compatibility of causal hidden-variable theories with a delayed-choice experiment, Phys. Rev. A **100**, 012114 (2019).

[36] E. Polino, I. Agresti, D. Poderini, G. Carvacho, G. Milani, G. B. Lemos, R. Chaves, and F. Sciarrino, Device-independent test of a delayed choice experiment, Phys. Rev. A **100**, 022111 (2019).

[37] Y. Ji, Y. Chung, D. Sprinzak, M. Heiblum, D. Mahalu, and H. Shtrikman, An electronic Mach–Zehnder interferometer, Nature (London) **422**, 415 (2003).

[38] R. Dumke, T. Müther, M. Volk, W. Ertmer, and G. Birkl, Interferometer-Type Structures for Guided Atoms, Phys. Rev. Lett. **89**, 220402 (2002).

[39] W. D. Oliver, Y. Yu, J. C. Lee, K. K. Berggren, L. S. Levitov, and T. P. Orlando, Mach-Zehnder Interferometry in a strongly driven superconducting qubit, Science **310**, 1653 (2005).

[40] A. D. Cronin, J. Schmiedmayer, and D. E. Pritchard, Optics and interferometry with atoms and molecules, Rev. Mod. Phys. **81**, 1051 (2009).

[41] J. W. Pan, Z. B. Chen, C. Y. Lu, H. Weinfurter, A. Zeilinger, and M. Żukowski, Multiphoton entanglement and interferometry, Rev. Mod. Phys. **84**, 777 (2012).